# OUR Z17 REDUCTION TECHNIQUE

Carl Heiles June 17, 2016

## ABSTRACT

We describe our observing technique and least-squares procedures to determine the opacity profile, the expected emission profile, and their uncertainty profiles. There are three procedures:

1. `z17_1.pro`, which solves for the optical-depth profile, the expected profile, and the first-order Taylor expansion of the HI emission in the sky.
2. `z17_2.pro`, which solves for the optical-depth profile, the expected profile, and the second-order Taylor expansion of the HI emission in the sky.
3. `fit_z17.pro` fits for a second or third order Taylor expansion and does not use the cold-sky antenna temp (called trcvr) in the fit. Rather, it assumes the continuum source contributes zero to the system temperature when you are not at the on position. This is probably better because trcvr is not predicted perfectly accurately. However, deteremining which is better needs some experimentation. The baselines probably need to be subtracted before using `fit_z17`—needs checking!

§0.3 discusses the differences between the latter two and which might be preferable for particular cases.

### 0.1. The Arecibo telescope and our Z17 Observing Pattern

The Arecibo telescope has a reflector fixed on the ground and points by moving the feed structure. This makes many characteristics of the beam change as a source is tracked. These changes are discussed by Heiles et al. (2001) and documented in more detail on Arecibo's website. We sampled two linearly polarized channels simultaneously, performing both auto and crosscorrelations with Arecibo's three-level "interim" digital correlator.

We observed each source by repeating our observational pattern. This pattern consists of 17 positions: one on-source and 16 off-source positions (Figure 1). It allows us to calculate and correct for the first and second derivatives of 21-cm line emission intensity on the sky. With 17 positions, we refer to this pattern as "Z17".

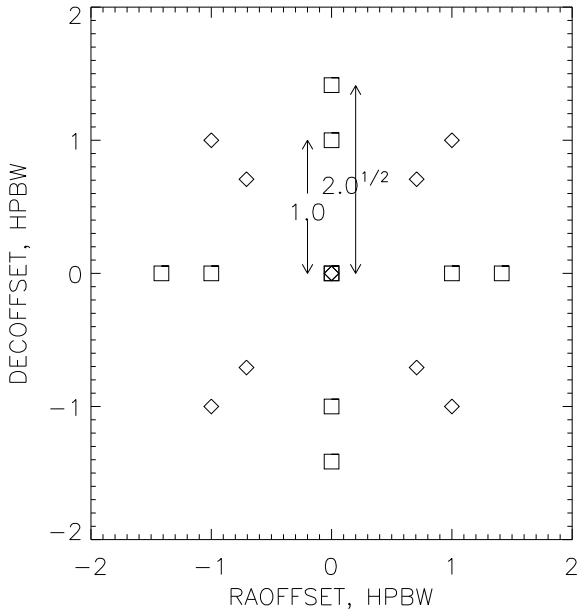


Fig. 1.— The 17-point measurement grid of the Z16 pattern. It consists of two crosses, one aligned with ra/dec (squares) and one at 45° to ra/dec (diamonds). The innermost points are 1.0 *HPBW* and the outermost points $2^{1/2}$*HPBW* from the central point.

In addition to the spatial derivatives, there are instrumental effects involving the system gain. The on-source antenna temperature can vastly exceed the off-source ones. With three-level correlators it is important to keep the input level near the optimum value; this meant that the electronics gains for the on-source measurements ($\mathcal{G}_n$ below) were set lower than those for the off-source ones ($G_n$ below). These gains had to be calibrated independently and have independent uncertainties. The instrumental effects that should be accounted for include:

1. The on-source electronics gain $\mathcal{G}$ for each pattern $n$ is not perfectly calibrated.

2. The off-source electronics gain $G$ for each pattern $n$ is not perfectly calibrated.

3. The on-axis gain of the telescope changes with $(az, za)$, so that the source deflection changes.

4. Arecibo's beam shape changes with $(az, za)$. In particular, the location of the first zero in the antenna beam response changes and, moreover, does not always exist. This

means that the off-source spectra contain some remnant of the source intensity so one cannot obtain the expected profile by going just a little way off source.

5. The intrinsic system temperature changes with $za$, particularly at high $za$ where the feed response spills over to onto the ground.

In the reductions for the Millennium survey (Heiles & Troland 2003), we accounted for all of these effects. Here, we use a simpler reduction technique, which only accounts for the last two above. We ignore the first three because the on-axis gain changes with $(az, za)$; accounting for it requires knowledge of the telescope gain and beam properties, which in any case are somewhat uncertain and also can change as the telescope surface errors increase gradually with time, or decrease when adjusted. We feel that the associated uncertainties make HT's original technique "overkill".

However, the fourth instrumental effect, the telescope's off-axis point-source response, is easy to evaluate from the off-line spectral baseline channels. And the fifth, the change in system temperature with $za$, depends only on the spillover onto the ground; this depends only on illumination pattern on the primary surface, which, in turn, depends only on the feed illumination pattern and the arrangement of the subreflectors. This means that this effect is stable in time. Moreover, it is easy to correct for.

### 0.2. Our Simpler Analysis Technique

To derive 21-cm absorption line spectra, one observes off-source positions to obtain the "expected profile" $T_E(\nu)$, which is the line profile one would observe at the source's position if the continuum source were turned off. One uses the expected profile for two purposes: one subtracts it from the on-source spectrum, which difference provides the opacity spectrum; and one combines it with the opacity spectrum to obtain the spin temperatures.

This conventional technique is not perfect because the off-source emission spectra differ from the expected profile. There are two reasons. First, the antenna response to the continuum source is not zero for the off positions, so the off-source emission spectra are contaminated by a small, unknown contribution from the opacity spectrum. Second, there is angular structure in the emission spectra. We treat these problems using a least squares technique.

We assume that the angular structure in each spectral channel can be represented by a Taylor series expansion. The Z17 pattern allows us to evaluate this expansion to second order. Within each pattern we have $J$ measurements, each of which is denoted by subscript

$j$. Each pattern consists of measurements at $J = 17$ positions, one of which is directly on-source; even the off-source positions have nonzero antenna temperature from the source, as discussed above. The symbols $(\nu)$ indicate frequency-dependent quantities within the profile; unsubscripted temperatures are continuum. Quantities to be derived from a least squares treatment are enclosed in square brackets. There are 7 such quantities for the full second-order expansion and 4 for the first-order one.

Thus, for each pattern we have the equations of condition

$$T_{A,j}(\nu) - T_{R,j} = [e^{-\tau(\nu)}]T_{C,j} + [T_E(\nu)] + \left[\frac{\partial T_E(\nu)}{\partial \alpha}\right] \Delta\alpha_j + \left[\frac{\partial T_E(\nu)}{\partial \delta}\right] \Delta\delta_j + \left[\frac{\partial^2 T_E(\nu)}{\partial \alpha^2}\right] \frac{(\Delta\alpha_j)^2}{2} + \left[\frac{\partial^2 T_E(\nu)}{\partial \delta^2}\right] \frac{(\Delta\delta_j)^2}{2} + \left[\frac{\partial^2 T_E(\nu)}{\partial \alpha \partial \delta}\right] (\Delta\alpha_j)\ (\Delta\delta_j)\ , \quad (1)$$

where $T_{A,j}(\nu)$ are the measured antenna temperatures, $T_{R,j}$ are the receiver temperatures (a function of $za$), $T_E(\nu)$ is the 21-cm line emission that would be observed in the absence of the source, $\Delta\alpha_j$ are the right-ascension offsets, and $\Delta\delta_j$ are the declination offsets.

$T_{C,j}$ are the antenna temperatures of the source (which are small except at the on-source position). We obtain these from the off-line "baseline" spectral channels.

### 0.3. First-order versus Second-order Taylor Expansion

There are two reduction programs. `z17_1.pro` solves for the first-order expansion, and `z17_2.pro` solves for the second order one. We recommend using both, comparing the results, and using the appropriate one for each particular case.

In principle, the second-order Taylor expansion is preferred because it can more accurately represent the true spatial variation of $T_E(\nu)$. However, its derived spectra for both $T_E(\nu)$ and $e^{-\tau(\nu)}$ are noisier than those derived from the first-order Taylor expansion. The excess noise occurs for two reasons:.

1. In the second-order expansion there are $P = 6$ unknown parameters derived from $M = 17$ measurements, in contrast to the first-order one where there are only $P = 3$ unknowns. The statistical noise is proportional to $(M-P)^{-1/2}$, so the former expansion is intrinsically noisier by $(14/11)^{1/2} = 1.13$.

2. More serious is the high covariance between the second derivatives of the expected profile and the $e^{-\tau(\nu)}$ and $T_E(\nu)$ spectra. For the second-order expansion, the typical

normalized covariance matrix (also known as the correlation matrix) for the unknowns in equation 1 is

$$\mathbf{ncov2} = \begin{bmatrix} 1.00 & -0.34 & 0.02 & -0.00 & 0.55 & 0.55 & 0.00 \\ -0.34 & 1.00 & -0.01 & 0.00 & -0.82 & -0.82 & -0.00 \\ 0.02 & -0.01 & 1.00 & -0.00 & 0.01 & 0.01 & 0.00 \\ -0.00 & 0.00 & -0.00 & 1.00 & -0.00 & -0.00 & 0.00 \\ 0.55 & -0.82 & 0.01 & -0.00 & 1.00 & 0.67 & 0.00 \\ 0.55 & -0.82 & 0.01 & -0.00 & 0.67 & 1.00 & 0.00 \\ 0.00 & -0.00 & 0.00 & 0.00 & 0.00 & 0.00 & 1.00 \end{bmatrix} \quad (2)$$

while that for the first-order expansion is

$$\mathbf{ncov1} = \begin{bmatrix} 1.00 & 0.56 & 0.01 & -0.00 \\ 0.56 & 1.00 & 0.01 & -0.00 \\ 0.01 & 0.01 & 1.00 & -0.00 \\ -0.00 & -0.00 & -0.00 & 1.00 \end{bmatrix} \quad (3)$$

The matrix **ncov2** exhibits high covariance (–0.82) between the interesting parameters ($T_E(\nu)$ and $e^{-\tau(\nu)}$) and the second derivatives ($\frac{\partial^2 T_E(\nu)}{\partial \alpha^2}$ and $\frac{\partial^2 T_E(\nu)}{\partial \delta^2}$). This contributes to the statistical noise.

Thus, we have a tradeoff: the second-order expansion is more accurate (smaller systematic errors), while the first-order one is more precise (smaller random errors). We illustrate these points with our results for a single pattern for 3C132. Figure 2. For $e^{-\tau(\nu)}$, the black (first order) and red (second order) fits differ significantly near $Vlsr = 15$ km/s; the second order fit should be more accurate.

## REFERENCES

Heiles, C. et al. 2001, PASP, 113, 1247.

Heiles, C. & Troland, T.H. 2003, ApJS, 145, 329

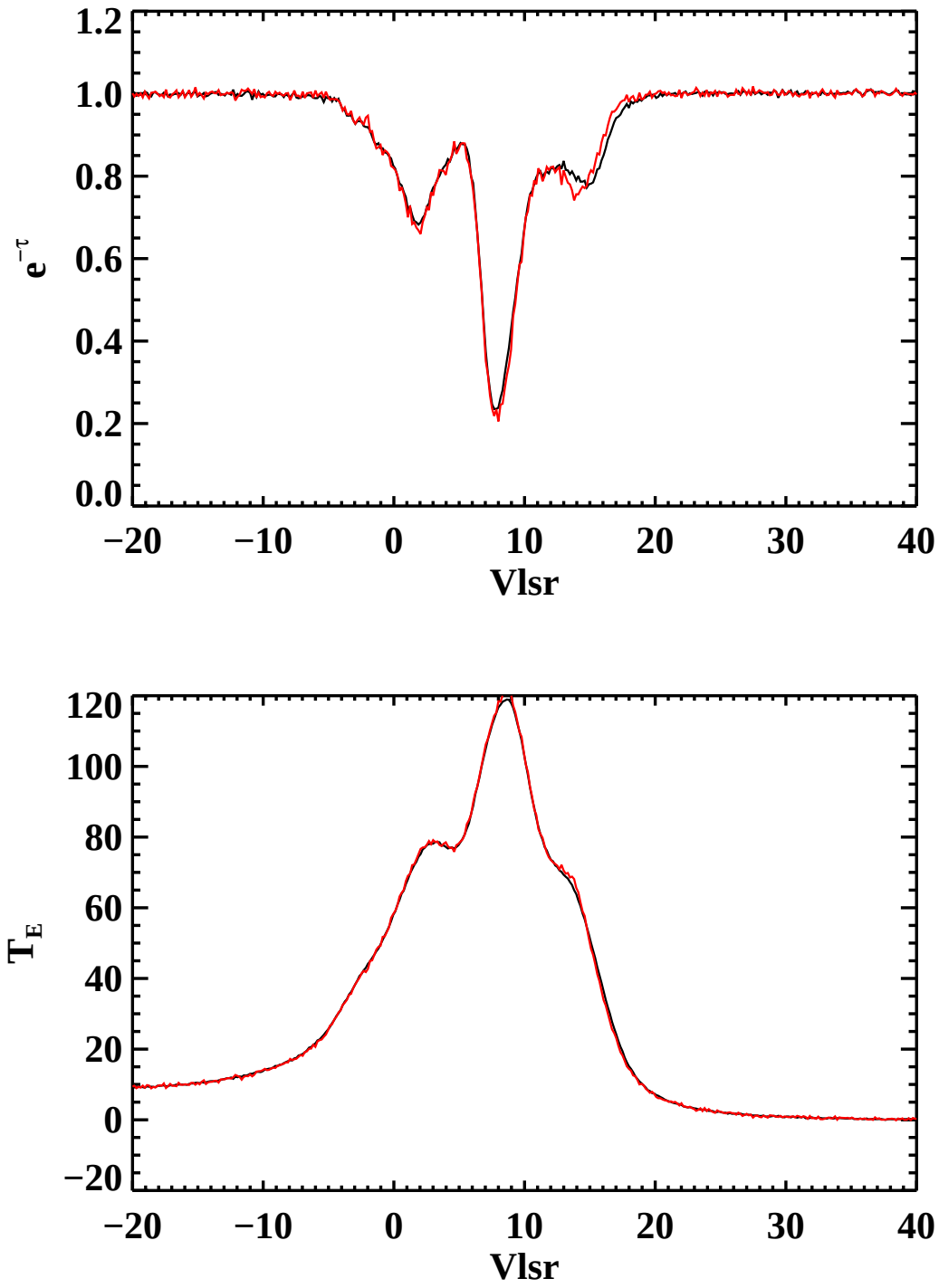


Fig. 2.— First-order (black) and second-order (red) fits for the $T_E(\nu)$ (bottom) and $e^{-\tau(\nu)}$ (top) profiles for 3C132.